

Advances in Fluid Interface-Atomic Force Microscopy

D. Eric Aston¹ and John C. Berg²

¹ University of Idaho, Chemical Engineering, P.O. Box 441021, Moscow, ID 83844-1021 USA

² University of Washington, Chemical Engineering, Box 351750, Seattle, WA 98195-1750 USA

Keywords: atomic force microscope; force profiles; fluid interface; film drainage; hydrodynamics; pull-off force; hydrophobic interaction.

Abstract. Several interaction studies have been successfully conducted between an oil droplet (n-hexadecane) and various glass microspheres in aqueous environments with the colloidal probe technique in an atomic force microscope (AFM). The methodology behind fluid interface (FI)-AFM for accurate interparticle force measurements is critically based on an exact model of droplet deformation. The hydrophobic interaction and hydrodynamics in a spherically wrapping thin film are investigated by parametrically changing external approach velocity and sphere radius. At closest approach, the true sphere-drop separation can be deconvoluted from experimental data without ambiguity. An increase in film stability is directly observed as a function of velocity between hydrophobized-glass and hexadecane, both in pure water and with the addition sodium dodecyl sulfate (SDS) below the critical micelle concentration (CMC). Theoretical force profiles are constructed from the augmented Young-Laplace equation modified to allow pseudo-steady state hydrodynamic drainage over two distinct regimes. Reynolds lubrication dominates in the limit of small droplet deformations. For an indented interface, a wrapping film condition of constant thickness and increasing extent is applied with zero drainage at the apex.

Introduction

Atomic force microscopy (AFM) is being used with increasing frequency for investigating particle interactions near fluid-fluid interfaces, specifically, for air bubbles [1-9] and hydrocarbon oil droplets [10-17] submerged in aqueous solutions. However, the standard atomic force microscope (also, AFM) is unable to measure the actual separation between the probe particle and these highly deformable interfaces. It is difficult, if even possible, to control bubble or drop deflections directly, but they may be either measured independently with instrument modifications [4] or extracted through theoretical deconvolution of force-distance data.

Both experiments and theoretical arguments have determined that bubbles and drops deformed by impinging rigid spheres are not exactly Hookean in nature, i.e., linear deflectors [16,18]. While, linear approximations [15,19-21] can be more than sufficient for characterizing the mechanical behavior of a flexible interface for some purposes, it is insufficient in many cases for truly accurate measurement of surface forces vs. actual separation.

By carefully designing parametric AFM experiments, two or more interaction parameters may be investigated with an appropriate theoretical model that converts force vs. scanner displacement data into force vs. surface separation. Fluid interface (FI)-AFM is only quantitatively successful when the experiments build from simple to more complex systems to limit the number of unknown variables in procession. Classic DLVO surface forces should be investigated first to prove experiment and model matching. Then, other long-range interactions may be unambiguously studied.

Overall, the extent of the changing drop profile depends mostly on probe radius, rather than Debye length, surface potentials or charges, Hamaker constant, approach velocity, or any other property. All droplet deformation corresponds to the applied force balancing the net effect of Laplace pressure in magnitude and direction along the interface. This pseudo-steady state condition is mediated via the

disjoining pressure of the thin film being squeeze between the interfaces. But long-range, or thick-film, hydrodynamics are expected to alter both the film thickness and the drop profile to a larger degree. The interfacial profile at a particular net force loading is calculated in a numerical procedure using the augmented Young-Laplace equation with the appropriate disjoining pressure terms and geometric constraints. The inclusion of hydrodynamics requires an iterative solution for the spherical colloid probe AFM [22] experiments to be fitted accurately.

The purpose of this work is to review the current status of FI-AFM, paying careful attention to the more difficult concepts being addressed in the extant literature. The importance of hydrodynamics in film drainage is emphasized, even for pseudo-steady state cases of AFM. The present analysis shows the need for rigorous mathematical treatment of the film drainage with bubbles and drops resulting in two hydrodynamic regimes: 1) large separation and small drop deflections, or weak interactions, 2) small separations and droplet dimpling—the strong interactions of a “wrapping film.” Experimental results with glass [17] and polystyrene [16] microspheres and n-hexadecane droplets in water are discussed for verification of the FI-AFM model. Both hydrophobic and hydrophilic probes were employed in several concentrations of sodium nitrate (NaNO_3) and sodium dodecyl sulfate (SDS) to vary electrostatic double-layer thickness and interfacial tension, respectively. Probe radius and external approach velocities were varied to explore hydrodynamic effects. Also, the first complete interfacial tension titrations with SDS are presented for glass against n-hexadecane with dynamic effects resolved above the CMC.

The FI-AFM geometrical setup is described by a rigid, spherical surface (the probe) applying force orthogonal to the apex of an infinitely deformable boundary, i.e., the drop or bubble (Fig. 1). The mathematical description of the fluid interface is represented by the curvature term in the augmented Young-Laplace equation (Eq. 1) with first and second derivatives of height with respect to radius, $z'(r)$ and $z''(r)$:

$$\mathbf{s} \left(\frac{z''(r)}{(1+z'(r)^2)^{3/2}} + \frac{z'(r)}{r\sqrt{1+z'(r)^2}} \right) = g\Delta \mathbf{r}z(r) - [P_o - \Pi(D(r))]. \quad (1)$$

The pressure due to the stress of deforming a boundary of surface tension \mathbf{s} (i.e., Laplace pressure) is equated with the sum of all applied pressure components at a location $z(r)$. Here, the pressure field includes gravity ($g\Delta \mathbf{r}z$), the initial internal drop pressure (P_o), and surface forces (Π).

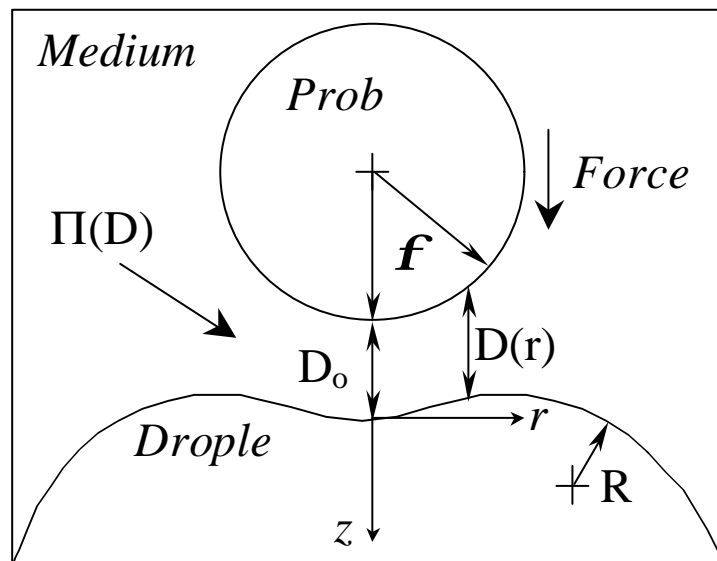


Figure 1: Schematic for AFM microsphere interacting axisymmetrically with a droplet (or bubble) separated by a liquid film of thickness $D(r)$ and radius of curvature R .

Gravity may be excluded in many cases without affecting the outcome, especially for low Bond number ($Bo = g\Delta\rho R^2/\sigma$). Since the curvature far from the deformation zone is effectively constant, P_o is also considered constant for a given drop or bubble: $P_o = 2\mathcal{S}R_d$. The separation profile, or aqueous film thickness, is $D(r)$, with closest approach occurring at the apex, $D(0) = D$. The drop profile (r,z) is numerically computed from Eq. 1 with a given composite pressure field for constraints of constant volume and symmetry ($dz/dr = 0$) [23-26].

For comparisons with experimental force-distance data, the disjoining pressure field, $\Pi(D(r))$, is summed over the interface to get the net vertical force, $F(z)$, where this z is the drop height and not to be confused with the scanner displacement. In application, the drop deformation will be the difference in AFM scanner and cantilever deflections minus the change in actual separation, ΔD . Since scanner motion is truly independent and the cantilever is undoubtedly an ideal spring, the issue of droplet or bubble linearity with applied force is elementary though tedious to prove. The only concern is whether a linear approximation is good enough for the specific goals of the study.

An oil-water interface should behave as a constant charge density surface [27] and glass spheres as constant potential surfaces [28]. DLVO terms for the pressure field include the usual non-retarded van der Waals and electrostatic double-layer interactions for dissimilar surfaces using the Debye-Hückel approximation (Eq. 2). The double-layer expression was derived from the potential energy equation shown by Kar *et al.* [29] between a constant potential surface (1) like glass and a constant charge density surface (2) like polystyrene or oil:

$$\Pi_{el} = \frac{2\epsilon\epsilon_0 k^2 [\mathbf{y}_{1o}\mathbf{y}_{2o} (e^{-kD} - e^{-3kD}) + (\mathbf{y}_{1o}^2 - \mathbf{y}_{2o}^2) e^{-2kD}]}{(1 + e^{-2kD})^2}. \quad (2)$$

There is excellent agreement with numerical solutions to the non-linear Poisson-Boltzmann equation [30] well above the low surface potential restriction ($|\mathbf{y}_{io}| < 25$ mV). Independently measured zeta-potentials are generally substituted for the isolated surface potentials, \mathbf{y}_{1o} and \mathbf{y}_{2o} . Analogous relationships for two dissimilar constant potential surfaces are also found to be sufficient well above the Debye-Hückel weak interaction limit.

A net system curvature for the deforming surface, R , is recalculated for each separation step, and the approach velocity, dD/dt , is computed at increments along the interface, (r,z) , to allow for a non-zero hydrodynamic contribution as a pseudo-steady state term. Hydrodynamic drainage force scales with R^2 under Reynolds conditions and with R^3 for wrapping film conditions [31]. The Reynolds lubrication pressure (Eq. 3) is summed with the other surface pressure terms for the initial drop profile estimate at a given separation [32]:

$$\Pi_R = \frac{3\mathcal{H}R}{D^2} \frac{dD}{dt}. \quad (3)$$

Previous experiments have shown that even with high electrostatic screening (0.1 M NaNO_3) and minimized hydrodynamic repulsion ($dD/dt = 200$ nm/s) between polystyrene and hexadecane, the aqueous film is stable in the wrapping configuration in spite of an expected hydrophobic attraction [16]. An empirical surface interaction is added to Π in the event that DLVO theory does not predict long-range attractions between surfaces in water when at least one is hydrophobic [33,34]. An exponential convention for this ‘‘hydrophobic force’’ has been adopted while little understanding of the complex phenomena is revealed. Recent investigations have indicated a minimum of two distinct effects that manifest in hydrophobic experiments [35,36], but only a single function has been employed in the present study where long-range snap-ins dictate. The requisite pressure function has the common scalar, C_1 , and decay length, λ , which are independent of electrostatics:

$$\Pi_h = \frac{C_1}{2\mathbf{pl}} \exp\left(\frac{-D}{\mathbf{l}}\right). \quad (4)$$

A classic hydrophobic interaction [37] could remain unobserved in FI-AFM since the magnitude of interfacial tension is often not sufficient to rupture the intervening film at any loading.

Once the droplet has dimpled inward, the more appropriate hydrodynamic relationship within the newly wrapping film is that derived by Hartland and supported by microscopic observation of a paraffin film draining between an aluminum sphere and a glycerol interface [31]:

$$\Pi_H = \frac{12\mathbf{hR}_s^2}{D^3} \frac{dD}{dt} \log\left[\frac{1 + \cos \mathbf{f}}{1 + \cos \mathbf{f}_c}\right]. \quad (5)$$

The radius of the sphere, R_s , describes the curvature effect. The instantaneous extent of the wrapping film, \mathbf{f}_c , is defined by the location of the interfacial inflection point within the gap (Fig. 1). As the angle \mathbf{f} increases from 0 to \mathbf{f}_c , the separation increases very slightly and the thinning velocity decreases. Only the first term of Hartland's original pressure equation has been used here to eliminate redundancy in accounting for gravity (Eq. 1).

No-slip boundaries, parallel film flow and Newtonian fluid assumptions are made, though recent theoretical developments suggest hydrophobic surfaces may allow limited slip [38]. Reynolds theory is more reasonable for the *thick-film regime* as defined for FI-AFM as a positive interfacial curvature (i.e., no dimple), which generally corresponds with large separations and weak interactions [17]. Very little interfacial deflection occurs while the drop has positive curvature in the thick-film regime, so the rigid sphere-plate interaction implied by the Reynolds lubrication equation is an adequate approximation. Of course, the drop radius of curvature does change and the interface deflects nonlinearly in this mode as well as when dimpled, but the deviation from a Hookean spring is much less significant allowing its reasonable usage for thick-film drainage as defined here. After the droplet flattens at the apex and begins dimpling, Eq. 5 replaces Eq. 3 within the wrapping film, i.e., the *thin-film regime*, but the hydrodynamic repulsion outside of the film ($\mathbf{f} > \mathbf{f}_c$) is not zero at \mathbf{f}_c . Of course, the hydrodynamic transition from the first drainage regime to the second is a smooth process in reality. The numerical value of Π_H is a pressure drop relative to Π_R , which is relative to the pressure far away from both interfaces, viz., the bulk fluid pressure.

Results and Discussion

Physical deformation at the drop apex redistributes volume away from the axis, which is intuitively a nonlinear event. Using rigid spheres as probes that are orders of magnitude smaller than the droplet radius, R_d , has several consequences for FI-AFM. Most obvious is the fact that initial curvature of the interface plays a very small role in overall modeling force-distance profile, $F(z)$, results. This results in relatively high local disjoining pressures that can be sustained by the interface via Laplace pressure, which in turn means the minimum or "limiting" film thickness will be correspondingly small. Decreasing probe radius reduces hydrodynamic effects and allows a greater range of true separations to be accessible.

Interaction profiles are plotted in the familiar F/R vs. a distance scale, where the net force has been normalized by the probe radius, R , for convenience. Experimental $F(z)$ data were acquired with an AutoProbe® CP (ThermoMicroscopes, Sunnyvale, CA) using glass and polystyrene microspheres with radii in the range 0.8-50 μm (1-3 nm rms roughness) from Duke Scientific Corp. glued to triangular cantilevers (~ 0.05 N/m). Force sensitivity in solution was better than 0.1 nN. The horizontal alignment of the probe to within 10 μm of the n-hexadecane (oil) droplet apex ($R_d = 2500$ μm) was sufficiently close. Model results were plotted against the predicted scanner displacement, which was the sum of vertical deformation of the oil/water interface from its undisturbed state, Δz , and separation at the apex, D_0 . Both theory and experiment produce a nonlinear "constant compliance" region for the deforming oil-water

interface that does not allow the simplistic Hookean spring description (e.g., $F = k\Delta x$) to be sufficient for determining interaction parameters [16-18]. Increasing the force applied to the droplet causes an interfacial displacement that is not proportional. The oil-water interface gradually stiffens with increasing deflection; its “spring constant” is not constant.

When DLVO interaction parameters were known or measured [35], only two hydrophobic parameters would be fitted, if necessary, since the hydrodynamic parameters (dD/dt , \mathbf{f}_c , and \mathbf{f}) are calculated throughout the model from the initial conditions, stepping through values of separation, D . Force measurements against an oil droplet were reported [17] for a few sphere sizes (R_s of 0.8, 7, 15, and 50 μm) submerged in 99% pure sodium dodecyl sulfate (SDS) solution at 7 mM (CMC = 8 mM @ $T = 22^\circ\text{C}$) for scanner speeds of 2, 5, 10, and 20 $\mu\text{m/s}$. The external driving velocity of the scanner is the only parameter that directly changes film drainage without permanently altering the system conditions. However, when the AFM drive velocity increases, the effect on drainage rate is reduced due to more rapid interfacial deflection.

With the oil-water interfacial tension reduced from 52 mN/m (pure oil-water) to approximately 8 mN/m, the droplet deforms more easily against applied pressure and will maintain a larger separation between itself and the probing glass sphere. Also, the surface charge density increased, so the electrostatic repulsion was even more significant and the hydrophobicity was reduced. The thicker double-layer increases stability against coalescence. SDS does not adsorb very strongly to clean silica surfaces [39], so its electrostatics condition should be changed very little. But other hydrophobic interfaces will take up significant amounts of SDS, though perhaps not complete monolayers [6]. Without exact values for the increased surface charge densities, the film thickness cannot be determined with precision.

Two intriguing possibilities for FI-AFM were alluded to in previous publications but remain undeveloped for future quantitative investigations: 1) the direct experimental determination of final film thickness with information from reversible hydrodynamic pull-off forces [17], and 2) the measurement of local, dynamic interfacial tensions for observation of Gibbs elasticity and Marangoni phenomena [16,17]. While both goals have yet to be explored thoroughly, the AFM has already demonstrated its capability for gather such data. Once the appropriately sophisticated models have been developed, the relatively straightforward experimental results of force and displacement with time may be interpreted.

The first experiment, for finding accurate separation limits, was conducted with the largest glass sphere for best resolution of hydrodynamic repulsion. The largest glass sphere ($R_s = 50 \mu\text{m}$) was used for hexadecane droplet in 10 mM SDS solution (above the CMC) for the most stable interfacial conditions. Figure 2 shows consecutive pull-off measurements where the scan velocity was increased over one order of magnitude (2-20 $\mu\text{m/s}$). Since the net force at a given separation increases with velocity, the oil interface deformation also increases such that the closest approach is accomplished at 2 $\mu\text{m/s}$ where hydrodynamic effects are minimized but not negligible. Experiments with smaller probes ($R_s = 15 \mu\text{m}$) suggested that the pull-off attraction indeed varies microsphere radius as expected [17]. This type of parametric experiment should be able to independently verify the limiting separation achieved from that predict with the above model for

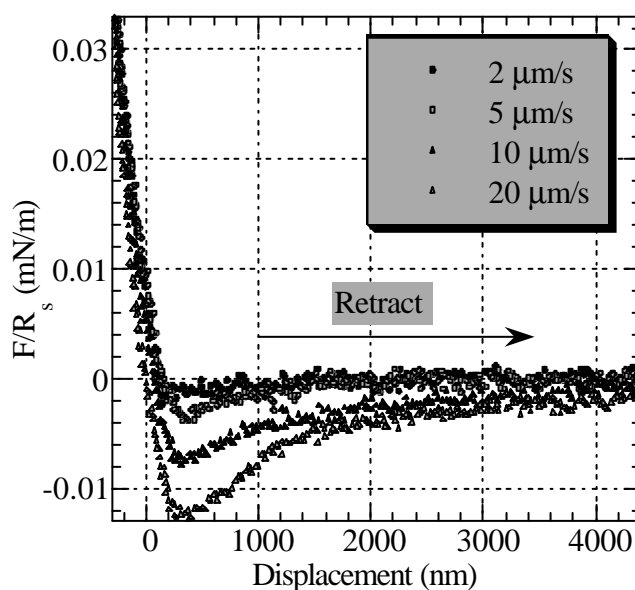


Figure 2: Hydrodynamic attraction during pull-off measurements of a 50 μm glass sphere retracting from a hexadecane droplet in 10 mM SDS solution at varied rates.

approaching interactions. A second kind of measurement was performed on the same system where pull-offs were collected at the same speed (20 $\mu\text{m/s}$) but at different absolute separations. Results show an increasing hydrodynamic attraction during retraction when the closest point achieved on approach decreases. After each profile was acquired, the probe was advanced 100 nm closer to the resting droplet. At relatively large separations (1st pull-off), the droplet barely exhibits any interaction with the probe. Further advancing of the probe after the 4th measurement does not show an increase in pull-off force, suggesting that the limiting separation was reached for these conditions.

All hydrodynamic pull-off curves must be plotted on an arbitrary displacement scale because the true separation is indeterminate without proper deconvolution of interfacial deformation. In order to magnify the differences in the data, the maximum $F(z)$ slope was subtracted from all curves. This manipulation does not reproduce a vertical "hard wall" at small separations but a slightly curving trend, further demonstration that the droplets do not behave as linear deflectors with applied force. The film never ruptured during the experiments and pull-off profiles show the hydrodynamic attraction disappearing for slower scan speeds.

Conclusions

The complexities involved in deconvoluting experimental FI-AFM data for quantitative interfacial studies is prohibitive to its quick application in other fields and with other systems. However, the present examples in the literature clearly show that this field of investigation will be extremely powerful when the appropriate modeling tools have been constructed for data analysis. The nature of current AFM force profiling techniques requires that hydrodynamic film drainage be carefully measured and theoretically understood for the appropriate configurations. With a probe sphere impinging against a deforming droplet or bubble, there are at least two distinct hydrodynamics regimes described adequately by Reynolds lubrication and Hartland's wrapping film drainage approximations. These correspond to larger and smaller separations, or weak and strong interactions, respectively, and are often significant under normal AFM probing speeds. Furthermore, hydrodynamic pull-off force profiles provide a direct experimental avenue for the determination of final film thickness for systems that do not coalesce, if the fluid flow in this attractive regime can be adequately modeled.

When the hydrodynamics are well understood and the classic DLVO interaction parameters are known and independently measurable, FI-AFM may be used to investigate other surface forces that have unknown interaction parameters, e.g., hydrophobic attractions or other phenomena like steric repulsion or Gibbs elasticity. Preliminary dynamic results demonstrate that FI-AFM is sensitive to interfacial stiffness changes that may correspond to transient surface adsorption and desorption of surfactant. With an appropriate theoretical relationship, local dynamic interfacial tensions are accessible with a standard AFM.

Acknowledgements

The authors gratefully acknowledge the financial support of the Center for Surfaces, Polymers, and Colloids at the University of Washington.

References

- [1] H.-J. Butt: *J. Colloid Interface Sci.* Vol. 166, (1994), p. 109.
- [2] W.A. Ducker, Z. Xu and J.N. Israelachvili: *Langmuir* Vol. 10, (1994), p. 3279.
- [3] M.L. Fielden, R.A. Hayes and J. Ralston: *Langmuir* Vol. 12, (1996), p. 3721.
- [4] E.V. Thompson. Review of Flotation Research. In *Paper Recycling Challenge - Deinking & Bleaching*; Vol. II; Doshi, M. R., Dyer, J. M., Eds.; (Doshi & Associates, Inc., Appleton, WI, 1997), p. 31.
- [5] S.R. Berg, F.G. Paulsen, J.C. Hassler and E.V. Thompson. "Force-Distance Measurements of Bubble/Particle Interactions"; 4th Research Forum on Recycling, 1997, Quebec, Qc, Canada.
- [6] M. Preuss and H.-J. Butt: *Langmuir* Vol. 14, (1998), p. 3164.
- [7] M. Preuss and H.-J. Butt: *Int. J. Miner. Process.* Vol. 56, (1999), p. 99.
- [8] J. Ralston, D. Fornasiero and R. Hayes: *Int. J. Miner. Process.* Vol. 56, (1999), p. 133.
- [9] S. Ecke, M. Preuss and H.-J. Butt: *J. Adhesion Sci. Technol.* Vol. 13, (1999), p. 1181.
- [10] S. Basu and M.M. Sharma: *J. Colloid Interface Sci.* Vol. 181, (1996), p. 443.
- [11] P. Mulvaney, J.M. Perera, S. Biggs, F. Grieser and G.W. Stevens: *J. Colloid Interface Sci.* Vol. 183, (1996), p. 614.
- [12] B.A. Snyder, D.E. Aston and J.C. Berg: *Langmuir* Vol. 13, (1997), p. 590.
- [13] D.E. Aston and J.C. Berg: *J. Pulp Paper Sci.* Vol. 24, (1998), p. 121.
- [14] P.G. Hartley, F. Grieser, P. Mulvaney and G.W. Stevens: *Langmuir* Vol. 15, (1999), p. 7282.
- [15] G. Gillies, C.A. Prestidge and P. Attard: *Langmuir* Vol. 17, (2001), p. 7955.
- [16] D.E. Aston and J.C. Berg: *J. Colloid Interface Sci.* Vol. 235, (2001), p. 162.
- [17] D.E. Aston and J.C. Berg: *Ind. Eng. Chem. Res.* Vol. 41, (2002), p. 389.
- [18] D. Bhatt, J. Newman and C.J. Radke: *Langmuir* Vol. 17, (2001), p. 116.
- [19] D.Y.C. Chan, R.R. Dagastine and L.R. White: *J. Colloid Interface Sci.* Vol. 236, (2001), p. 141.
- [20] P. Attard and S.J. Miklavcic: *Langmuir* Vol. 17, (2001), p. 8217.
- [21] P. Attard and S.J. Miklavcic: *J. Colloid Interface Sci.* Vol. 247, (2002), p. 255.
- [22] W.A. Ducker, T.J. Senden and R.M. Pashley: *Nature* Vol. 353, (1991), p. 239.
- [23] S.J. Miklavcic, R.G. Horn and D.J. Bachmann: *J. Phys. Chem.* Vol. 99, (1995), p. 16357.
- [24] R.G. Horn, D.J. Bachmann, J.N. Connor and S.J. Miklavcic: *J. Phys. Condens. Mat.* Vol. 8, (1996), p. 9483.
- [25] D.J. Bachmann and S.J. Miklavcic: *Langmuir* Vol. 12, (1996), p. 4197.
- [26] S.J. Miklavcic: *Phys. Rev. E* Vol. 54, (1996), p. 6551.
- [27] J. Lyklema. Fundamentals of Electric Double Layers in Colloidal Systems. In *Colloidal Dispersions*; Goodwin, J. W., Ed.; (The Royal Society of Chemistry, London, 1982), p. 47.
- [28] R.J. Hunter: *Foundations of Colloid Science*, Vol. 1; ; (Oxford University Press, New York, 1987).
- [29] G. Kar, S. Chander and T.S. Mika: *J. Colloid Interface Sci.* Vol. 44, (1973), p. 347.

- [30] D. McCormack, S.L. Carnie and D.Y.C. Chan: *J. Colloid Interface Sci.* Vol. 169, (1995), p. 177.
- [31] S. Hartland: *J. Colloid Interface Sci.* Vol. 26, (1967), p. 383.
- [32] D.Y.C. Chan and R.G. Horn: *J. Chem. Phys.* Vol. 83, (1985), p. 5311.
- [33] R.-H. Yoon, D.H. Flinn and Y.I. Rabinovich: *J. Colloid Interface Sci.* Vol. 185, (1997), p. 363.
- [34] E.A. Vogler: *Adv. Colloid Interface Sci.* Vol. 74, (1998), p. 69.
- [35] D.E. Aston and J.C. Berg: *Colloids Surf. A* Vol. 163, (2000), p. 247.
- [36] O.I. Vinogradova, G.E. Yakubov and H.-J. Butt: *J. Chem. Phys.* Vol. 114, (2001), p. 8124.
- [37] J.N. Israelachvili and R.M. Pashley: *Nature* Vol. 300, (1982), p. 341.
- [38] O.I. Vinogradova: *Langmuir* Vol. 11, (1995), p. 2213.
- [39] A. Thibaut, A. Misselyn-Bauduin, J. Grandjean, G. Broze and R. Jérôme: *Langmuir* Vol. 16, (2000), p. 9192.